Anonymous Referee #2:

We would like to thank the reviewer for the valuable and constructive comments, which helps us to improve the manuscript. Listed below are our responses to the comments point-by-point, as well as the corresponding changes made to the revised manuscript. The reviewer's comments are marked in black and our answers are marked in blue, in which the revision in the manuscript is further formatted as '*Italics*'.

1. Summary

The article by Zhang et al. retreads a lot of information already covered in Zhang et al. (AMT, 2016), with some additional analysis. Overall, I find there are potentially some interesting components of this paper that go beyond the author's previous work, but at the same time there are a number of aspects that are presented as novel insights that are either not sufficiently justified or explained, or are simply wrong. I cannot recommend this paper for publication. The authors should work to truly distinguish it from their previous work. My specific comments follow below (in chronological order, mainly).

Response: We thank the reviewer for raising this question and we hope that the reviewer will be convinced after our detailed clarification below.

(1) Although based on the same data sets as in the current manuscript, the previous paper "Measuring the morphology and density of internally mixed black carbon with SP2 and VTDMA" by Zhang et al. (AMT, 2016) specifically focused on:

- demonstrated an technical approach to determine the effective density of black carbon (BC) cores for internally-mixed BC particles (hereafter named as 'thick-coated BC particles' following the reviewers' suggestion) by a combined system of Single Particle Soot Photometer (SP2) and Volatility Tandem Differential Mobility Analyzer (VTDMA).

The effective density of BC cores for the thick-coated (internally-mixed) BC particles obtained in the previous work is then used in this work to calculate optical size of thick-coated (internally-mixed) BC particles. In the current study, we

- presented the general feature of the BC mixing state: number/mass fraction, diurnal variation, turnover rate, and coated thickness at a polluted sub-urban area of Beijing, China, in summer time;
- validated the sizing ability of SP2 (from ~200 nm to 400 nm) for both BC containing particles and scattering particles and further explored the possibility of using LEO-fit method and Mie calculation to extend its sizing ability towards larger size range (i.e., from ~400 nm up to ~550 nm, usually the SP2 scattering signal becomes saturated for the particles with diameter larger than 400 nm); Note that, previously the LEO-fit is usually used for the BC-containing particles to retrieve the original size of the particles and coated thickness (e.g., Gao et al., 2007; Schwarz et al., 2008; Laborde et al., 2013).
- compared the size distribution of the refractory BC from SP2 with that of non-volatile cores from VTDMA at 300 ℃, revealing a large fraction of low volatile non-BC components at Xianghe even at this high temperature.

The above major results have not been included in the AMT paper, and we feel that the two papers are readily distinguishable. It would be helpful if the reviewer could kindly specify the content that he/she considered as republishing, we may then further clarify it in more details.

(2) To sharpen the manuscript and present the scientific questions more clearly, we intensively revised the manuscript according to both reviewers' comments and suggestions (see attached the tracking change version of the revised manuscript), especially modified the abstract, the last paragraph of the Introduction section, the Methods section with a schematic plot of the data processing flow, and reorganized the Results and Discussion section 3.1, as made the following changes:

- The abstract now read as "*Black carbon (BC) particles in the atmosphere play*

an important role in regulating the earth's climate and their climate effects strongly depend on the mixing state. During the CAREBeijing 2013 campaign, we measured the size-resolved mixing state of BC-containing particles at 200, 250, 300 and 350 nm at a regional site (Xianghe, ~60 km to the south of Beijing) in the North China Plain (NCP) from 8 to 27 July 2013, by combining a single particle soot photometer (SP2) and a volatility tandem differential mobility analyzer (VTDMA). The SP2 measurements showed a clear two-mode distribution of the 'lagtime', based on which the BC-containing particles were classified into the 'thin-coated (or bare)' and 'thick-coated' BC particles. With similar method proposed in our previous study (Zhang et al., 2016), we found that the thin-coated (or bare) BC particles at 200-350 nm exhibited an irregular shape with fractal dimension of ~2.23 and very low effective density of about 0.25-0.45 g cm^{-3}. The average refractive index (RI) of the non-BC particles was retrieved to be ~1.42 by matching their optical size and mobility size pre-selected by the VTDMA. Here, only the unsaturated scattering signals of SP2 (i.e., particles with smaller than ~400 nm) were used in the retrieval and the obtained RI was found to be almost size independent, which was then applied as the RI of the non-BC coating materials of the BC-containing particles. For the thick-coated BC particles, the effective density (1.2 g cm^{-3}) and refractive indices (1.67-0.56i) of the BC core were adopted from Zhang et al. (2016). Based on the above parameters and the BC mass and particle scattering cross-section measured by the SP2, the optical sizes of the thick-coated BC-containing particles as well as the large non-BC particles with saturated scattering signal were derived with the leading-edge-only (LEO)-fit method and Mie calculation. We show a very good agreement between the optical particle diameter and the mobility diameter for the large non-BC particles (diameter > ~400 nm), as well as for the thick-coated BC particles. With our approach, the upper sizing detection limit of the SP2 can be extended by from ~400 nm to ~550 nm.

During the measurement campaign, we found that the non-BC particles

contributed ~85-90% of the total aerosol numbers in the size range of 200 nm to 350 nm. The rest 10-15% of the particles contained BC, which were portioned out into thick-coated and thin-coated (or bare) BC particles by ~45% and ~55%, respectively. The number fraction of thick-coated BC in total BC-containing particles (F_{In-BC}) shows pronounced diurnal cycles with a peak around noontime and an apparent turnover rate up to 6-9% h^{-1}. Such diurnal cycles are similar to the finding of Cheng et al. (2012), suggesting strong photochemical aging of BC particles and a competing effect of emissions and aging processes. The average coating thickness (CT) of the thick-coated BC particles (200-350 nm) was in the range of 74-108 nm, which increased with increasing particle size. Compared with an average CT of ~30 to ~60 nm in previous measurements in other less polluted locations, e.g., Long Island (NY, USA) in summer time (Sedlacek et al., 2012), Mexico City in spring time (Subramanian et al., 2010), Fukue Island (Japan) in spring time (Shiraiwa et al., 2008) and Weybourne (UK) in summer time (Liu et al., 2013), the observed thick-coated BC particles at Xianghe were more-aged, indicating fast secondary processes and strong light absorbing capacity of BC particles under the polluted conditions in the NCP. Moreover, our measurements revealed a large fraction of low-volatile non-BC components at 300 ℃. Above the incandescence detection limit of SP2 (BC particle diameter larger than ~70 nm), the refractory BC particles accounted for only 16-35% of residual particles measured by VTDMA at 300 ℃ in number. In such case, the assumption that the refractory residual materials at 300 ℃ are BC as in previous VTDMA studies (Philippin et al., 2004; Wehner et al., 2009; and Cheng et al., 2009) may cause significant overestimation of the number of internally mixed BC particles and on the other hand it may lead to an underestimation of the light absorption enhancement factors in NCP due to the remaining low-volatile non-BC materials coating on the BC particles after heated by the thermodenuder."

- At the end of the Introduction section, we added "*In this study, we measured*

BC mixing state combining SP2 and VTDMA techniques at a polluted sub-urban area of Beijing, China, in summer time. We first validated the sizing ability of SP2 (from ~200 nm to ~400 nm) for both BC-containing particles and non-BC particles and further explored the possibility of using LEO-fit method and Mie calculations to extend its sizing ability towards larger size range (i.e., from ~400 nm up to ~550 nm). Based on the particle size information, we then presented the general feature of the mixing state of BC-containing particles: number/mass fraction, diurnal variation, turnover rate, and coating thickness. At last, we compared the size distribution of BC cores from SP2 with that of non-volatile cores from VTDMA to explore the existence of the low volatile non-BC components at 300 ℃. "

- We add the following plot in Methods section:
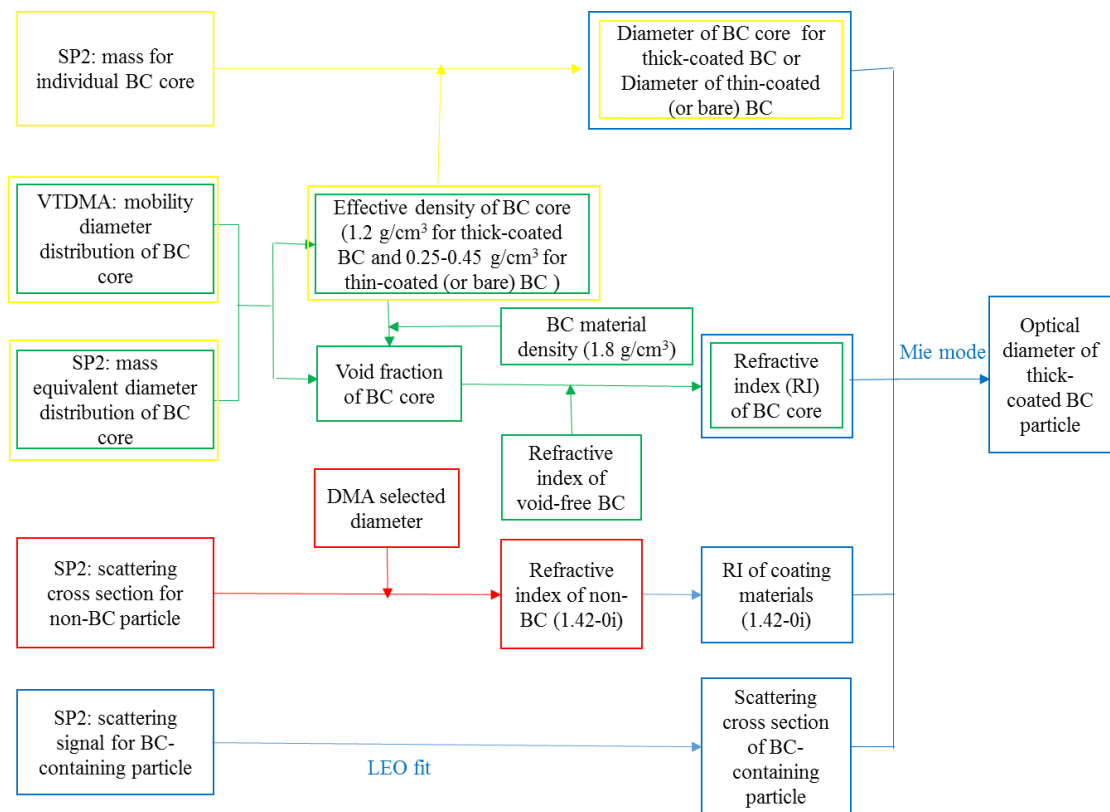
Fig. R1 (Figure. 2 in the revised manuscript). The data processing and analysing procedure in this study.

- We reorganized section 3.1 into *3.1 Morphology and effective density of the thin-coated (or bare) BC particles and 3.2 Particle optical size derived from*

SP2 (3.2.1 Non-BC particles with diameter larger than ~400 nm, 3.2.2 Thick-coated BC-containing particles).

2. Specific comments

(1) Consideration of the PSL's in Fig. 2 demonstrates that the observation of a wide band of refractive index values is a result of variability in particles passing through the SP2 laser and is not due to the distribution of diameters coming out of the DMA. This information can be translated into an effective uncertainty in the size of a given particle. Using the central RI value, a distribution of sizes can be constructed that would also reproduce the observed scatter. This should be considered. Very approximately, +/- 0.1 in RI space = +/- 20 nm in diameter space.

Response: Thanks to the reviewer for raising this concern. We, however, do not think that Fig. 2 is a result of variability in the particle passing through the laser. (1) The SP2 that we used in the field has been properly optically aligned and calibrated. The laser focus has been checked with beam-scan camera and showed one nice Gaussian distribution. (2) The diameter of PSL standard particles is usually centered at certain diameter with a distribution. Here we performed additional lab experiments to measure the number size distribution of the generated PSL standard particles (203 nm) with a Scanning Mobility Particle Sizer (SMPS, TSI 3936) and SP2. Figure R2 shows very similar normalized number size distribution of 203 nm PSL standard particles measured by SMPS (black curve) and SP2 (red curve). Thus, the distribution of PSL particles measured by SP2 in Figure 2 (Figure 3 in the revised manuscript) is not a result of variability in particles passing through the SP2 laser but rather the nature of the PSL standard particles, which corresponding to a span of refractive index of ~1.4 (~230 nm) to 1.8 (~180 nm) if all PSL particles are assumed to be 203 nm.
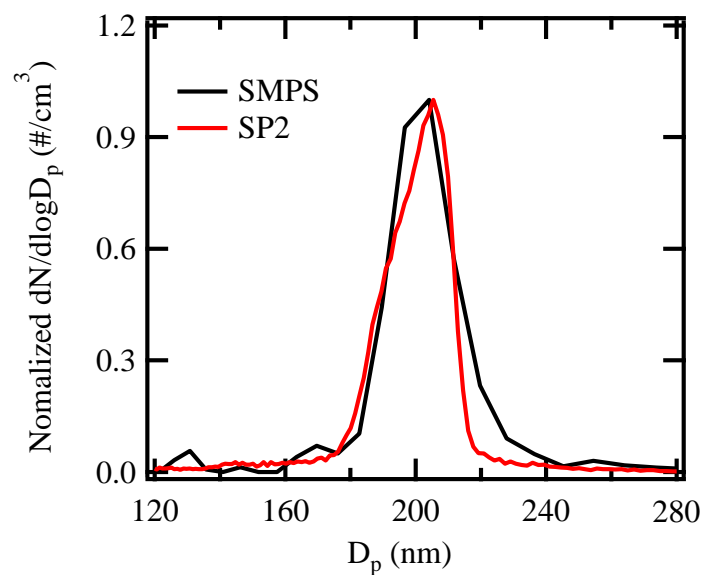
Fig. R2. (Fig. S2 in the revised manuscript) The size distribution of PBL at 203 nm using SMPS and SP2 measurements.

To make this point clear, we have added "*Noted that a well-defined particle size (203 nm) for PSL spheres still shows a wide size distribution. Fig. S2 shows very similar normalized number size distribution of 203 nm PSL standard particles measured by SMPS (black curve) and SP2 (red curve).This indicates that the RI distribution of PSL particles measured by SP2 in Fig. 3 is a result of the nature of the PSL standard particles, which corresponds to a span of refractive index of ~1.4 (~230 nm) to 1.8 (~180 nm) if all PSL particles are assumed to be 203 nm.*"

(2) Page 5: I have no idea what "bones and flesh" means. This is not at all common scientific language, nor is it clear in the usage.

Response: Thanks for the comment and the metaphor that we are using here may not be appropriate. We hope the revised description "*the voids among carbon spherules are filled by non-BC materials*" is clearer to the reviewer.

(3) Eqn. 6: It is unclear where this equation comes from. It appears to be made up by the authors. Does the use of this equation have a justification? I don't see how this is

physically justifiable.

Response: Thanks. This equation has been widely used in previous studies (e.g., Hänel, et al. 1968; Marley et al., 2001; Bond and Bergstrom, 2006; Schkolnik et al., 2007) to calculate the volume averaged refractive index. That is, the refractive index of a mixture particle can be calculated as the volume weighted average of the refractive indices of all components, as $\widetilde{m} = \sum_i \widetilde{m}_i c_i$, where $\widetilde{m}$ is the refractive index of a mixture particle; $\widetilde{m}_i$ is the refractive index of particle species; c is the volume ratio of particle species;. For example, Schkolnik et al. (2007) calculated the refractive index of biomass burning aerosol as the volume average of the refractive indices of elemental and organic carbon. Also, Bond and Bergstrom (2006) determined the refractive index of fresh BC as the volume average of the refractive indices of void-free carbon (1.95–0.79i at 550 nm) and air (1.00–0.00i).

In our study, assuming spherical morphology of the thick-coated (internally-mixed) BC particles, the void ratio R$_{void}$ is the volume fraction of void. According to the above equation, the refractive index of the particles therefore can be calculated as Eq. (6).

To make this point clear, we have revised the description of Eq. (6) in the manuscript: "*To obtain the RI$_c$, we assume that carbon spherules and voids together make a spherical BC core and the voids among carbon spherules are filled by non-BC materials. The RI$_c$ was estimated as the volume-weighted average of the RI of void and carbon spherules as in Eq. (6) (Hänel, et al., 1968; Marley et al., 2001; Bond and Bergstrom, 2006; Schkolnik et al., 2007), marked green in Fig.2:*

$$RI_c = [n_{BC} \times (1 - R_{void}) + n_{nonBC} \times R_{void}] + [k_{BC} \times (1 - R_{void})] \qquad (6)$$

where n_{BC} and n_{nonBC} are the real parts of RI for the BC materials and non-BC components (n$_{nonBC}$ = 1.95 and n$_{nonBC}$ = 1.42); k_{BC} is the imaginary part of the refractive index for BC (k_{BC} = 0.79) (Bond and Bergstrom, 2006); Volume ration of voids in the BC core, R$_{void}$ (~0.30) is determined by the method introduced in Zhang et al. (2016)."

(4) I understand the idea of adjusting the RI for non-BC containing particles to match

with the selected mobility diameter, as it is not unreasonable to think that the non-BC containing particles are spherical. However, I do not understand the justification for this for BC-containing ("internally mixed") particles that are not necessarily spherical and for which the extent of sphericity is likely linked to the amount of coated material. The relationship between mobility diameter and actual particle size (characterized in some particular manner) will be dependent upon the particle shape. Thus, it is not clear how, for internally mixed particles, the tuning which the authors have done actually leads to an improvement in the estimated size. They have imparted some assumption regarding shape that has not been justified.

Response: Thanks for the comments. There might be some misunderstanding on the data process and analyzing procedure. Here, we make a chart (Figure R1) to illustrate the whole data processing and analysing procedure. For non-BC particles within the SP2 detection limit (200-400 nm), we matched the optical diameter to the electro-mobility diameter by tuning its refractive index (RI), marked red in Figure R1. The retrieved RI for non-BC particles (~1.42 - 0i) seems to be independent on particle size (Figure 3 in the manuscript). Thus, when retrieving the optical size for the non-BC particles larger than 400 nm (saturated scattering signals in SP2 measurement) using LEO-fit and Mie calculation, we applied the same RI (~1.42 - 0i). On the other hand, for the thick-coated (internally-mixed) BC particles, when retrieving its optical diameter with the LEO-fit method (Gao et al. 2007) and Mie calculation, we did not adjust RI for either BC core or coated materials. In data process, RI for coated material was assumed to be same as the RI of non-BC particles (fixed with ~1.42 - 0i). RI for BC core was estimated as the volume weighted average of the RI of void and BC as Eq. (6) in the manuscript, marked green in Figure R1. The diameter of BC core was calculated from the BC mass given by SP2 and the predefined BC effective density (1.2 g/cm^3), marked yellow in Figure R1. The volume of void in the BC core and the BC core effective density (1.2 g/cm^3) are determined by the method introduced in Zhang et al. (AMT, 2016). After getting the diameter and RI of BC core, RI of coated material and the scattering signal of BC-containing particles from SP2,

we used LEO-fit combined with Mie model to retrieved the optical diameter of thick-coated particles (marked blue in Fig. R1).

In the Mie calculation, spherical shape was assumed for thick-coated (internally mixed) BC particles. We agree with the reviewer that the BC-containing particles are not necessarily spherical. However, as can be seen in Fig. 3B, the optical diameter of the thick-coated (internally-mixed) BC particles derived with the LEO-fit method agrees very well with their mobility diameter, which implies that the assumption on a spherical particle in Mie model calculation can be used for thick-coated BC particles in our case.

To make this point clear, we have revised the Sect. 2.2.3 in the manuscript: "*The optical sizes of the thick-coated BC-containing particles and the non-BC particles, especially those with saturated scattering signal in SP2, are retrieved using LEO-fit method (Gao et al. 2007) and Mie calculation. To determine the optical diameter of the non-BC particle ($D_{opt,non-BC}$), its scattering cross section (C_s) and the refractive index (RI_{non-BC}) of non-BC components should be known, as in the relationship (3) (Bohren and Huffman, 1983):*

$$D_{opt,non-BC} \sim (C_s, RI_{non-BC}), \qquad\qquad (3)$$

Here, C_s was determined by the LEO-fit method. As shown in the red colored flow in Fig. 2, RI_{non-BC} was determined through a closure study, where we matched the optical diameter of non-BC particle to the electro-mobility diameter of the mono-dispersed particles selected by DMA1 (200-350 nm, with unsaturated scattering signals in SP2) by tuning its refractive index. Since a DMA selects only quasi-monodispersed particles due to the width of the transfer function (Wiedensohler et al., 2012), the diameter of the selected particles shows a distribution rather than a single value of the nominal mobility diameter, which results in a more widely distributed RI_{non-BC} (~1.2-1.6). In this study, we took only the averaged peak value of each distribution for further calculations, which corresponds to the peak of the DMA transfer function. Figure 3 shows the retrieved RI_{non-BC} at different mobility diameters and we found that during the whole measurement period, the retrieved RI_{non-BC} values are almost size

independent with an average of ~1.4209. This RI_{non-BC} value is then used for the optical size retrieval of the larger non-BC particles with saturated scattering signals in SP2. We also applied this method to the polystyrene latex (PSL) spheres with well-defined particle size (203 nm). As shown in Fig. 3, the inversion gives a peak RI of 1.5861, very close to the RI of PSL (1.59) given in the literature (Gao et al., 2007). Noted that a well-defined particle size (203 nm) for PSL spheres still shows a wide size distribution. Fig. S2 shows very similar normalized number size distribution of 203 nm PSL standard particles measured by SMPS (black curve) and SP2 (red curve). This indicates that the RI distribution of PSL particles measured by SP2 in Fig. 3 is a result of the nature of the PSL standard particles, which corresponds to a span of refractive index of ~1.4 (~230 nm) to 1.8 (~180 nm) if all PSL particles are assumed to be 203 nm.

For the thick-coated BC particle, its optical size is determined from its scattering cross section (C_s), the diameter of the BC core (D_c) and the refractive index of BC core (RI_c) and coating material (RI_{cm}), as in the relationship (4):

$$D_{opt,In-BC} \sim (C_s, D_c, RI_{cm}, RI_c) \sim (C_s, M, \rho_{eff}, RI_{non-BC}, RI_c), \qquad (4)$$

In this study, RI_{cm} is equal to RI_{non-BC} (1.42 - 0i), assuming that coating materials on the BC core have the same chemical compositions as the non-BC particles. D_c is calculated from the BC mass determined by the incandescence signal of SP2 and the effective density of the BC core (1.2 g/cm³, retrieved in the study of Zhang et al. 2016b) as Eq. (5). These procedures are marked yellow in Fig. 2.

$$D_c = (\frac{6m}{\pi \rho_{eff}})^{\frac{1}{3}}, \qquad (5)$$

To obtain the RI_c, we assume that carbon spherules and voids together make a spherical BC core and the voids among carbon spherules are filled by non-BC materials. The RI_c was estimated as the volume-weighted average of the RI of void and carbon spherules as in Eq. (6) (Hänel, et al., 1968; Marley et al., 2001; Bond and Bergstrom, 2006; Schkolnik et al., 2007), marked green in Fig.2:

$$RI_c = [n_{BC} \times (1 - R_{void}) + n_{nonBC} \times R_{void}] + [k_{BC} \times (1 - R_{void})]i, \qquad (6)$$

where n_{BC} and n_{nonBC} are the real parts of RI for the BC materials and non-BC

components (n_{BC} = 1.95 and n_{nonBC} = 1.42); k_{BC} is the imaginary part of the refractive index for BC (k_{BC} = 0.79) (Bond and Bergstrom, 2006); Volume ration of voids in the BC core, R_{void} (~0.30) is determined by the method introduced in Zhang et al. (2016).

Based on the diameter and RI of the BC core, RI of coating material and the scattering signal of thick-coating BC particles from SP2, we used LEO-fit method (Gao et al., 2007) combined with Mie model to retrieved the optical diameter of thick-coating BC particles, marked blue in Fig. 2. As in previous studies (Liu et al., 2013; Metcalf et al., 2013; Sedlacek et al., 2012), the mixing state of BC-containing particles is then characterized by the coating thickness ($CT=(D_p-D_c)/2$) and the shell/core ratio (D_p/D_c)."

(5) I do not find Fig. 3 useful. It would only be surprising if the agreement between the "optical" and "prescribed" diameters was bad, given that they have tuned the RI to make the two match. All the authors are showing is that their tuning has worked to make the Doptical match the Dmobility. Also, this is not a validation of the "assumption of spherical BC particle[sic] in the Mie model calculation." The authors have forced agreement, not demonstrated anything about sphericity. Their method says little about the method "accuracy" (P6, L16)?

Response: As explained in our response to comment 4, for thick-coated (internally-mixed) BC particles, we did not tune RI to force the agreement. RI for the coated materials was assumed to be same as that of non-BC containing particles, and RI for BC core was estimated as Eq. 6 in the manuscript. Therefore, the good agreement between the optical diameter derived from the LEO-fit method and the particle mobility diameter selected by the DMA implies that the assumption on a spherical particle in Mie model calculation can be used for internally mixed (thick-coated) BC particles in our case. To this end, we would like to keep Fig. 3B in the manuscript (Figure R3B in this response).

The comparison of optical sizing from 400 nm to ~550 nm in Fig. 3A (Figure

R3A in this response) can be taken as a validation of the LEO-fit method. For non-BC containing particles larger than 400 nm, the scattering signal in SP2 would have been saturated. That is why the 400 nm was usually taken as the upper sizing limit of SP2. The optical diameters of the large non-BC containing particles (from ~400 nm up to ~550 nm) were retrieved by LEO-fit method (Gao, et al., 2007). In Fig 3A (Figure R3A in this response), we can see that for those large particles (from ~400 nm up to ~550 nm) the retrieved optical diameters fit well with their mobility diameters. Therefore, we further demonstrate in that the optical diameters of the large particles (from ~400 nm up to ~550 nm) can be still retrieved from the LEO-fit method (Gao, et al., 2007). Therefore, we would like to keep Fig. 3A (Figure R3A in this response) in the manuscript.

To make the purpose of plot clearer, we mark the signal saturation point (~400 nm) as blue dashed line in Figure 3 (Figure 5 in the revised manuscript). We have revised the discussion on Fig. 3 in the manuscript (Figure 5 in the revised manuscript): "*3.2.1 Non-BC particles with diameter larger than ~400 nm*

The LEO-fit method introduced by Gao et al. (2007) has been commonly used to retrieve the optical size of the thick-coated BC containing particles. In this study, we adopted the LEO-fit method not only to retrieve the peak height of scattering signal for larger non-BC particles with saturated scattering signals (particle size larger than the upper sizing limit of SP2 (~400 nm), most of double or triple charged particles in our study), but also to re-determine the scattering peak heights of non-BC particles (<400 nm) with full Gaussian distribution of the scattering signals detected by SP2. The scattering cross-section can be then obtained according to the calibration of PSL particles with well-defined sizes. Afterwards, the Mie calculation is used to translate the scattering cross-section into optical particle size, where the refractive index of 1.42 is applied for all the non-BC particles (RI_{nonBC} = 1.42 - 0i).

Although we use the DMA1 of the VTDMA selected particles with diameter ranging from 200 to 400 nm, due to multiple charge, particles larger than 400 nm could also been selected with certain probabilities. We thus calculated the size of the

large particles with double or triple charges whose mobility size is 200, 250, 300 or 350 nm. In Fig. 5A, we show the comparison of the mobility particle size as if they have only single charge and their optical size derived from LEO-fit and Mie calculation for non-BC particles. The agreement of particles with mobility diameter smaller than ~400 nm is of no surprise, because the RI_{non-BC} was retrieved by matching the optical diameter of non-BC particle at 200-400 nm to their electro-mobility diameter (marked red in Fig. 2). However, since the retrieved RI_{non-BC} shows independency on particle diameter, we applied the same refractive index for the particle larger than 400 nm. It can be found that the optical size from 400 nm to ~550 nm particles also agreed very well with their mobility size as if they have only single charge. This demonstrates that the optical diameters of the large particles (from ~400 nm up to ~550 nm) can be still retrieved from the LEO-fit method (Gao, et al., 2007).

3.2.2 Thick-coated BC-containing particles

Similar to the non-BC particles, the optical particle diameter of thick-coating BC particles derived from the LEO-fit method and Mie calculation (Fig. 2) showed an excellent agreement with their mobility diameter selected by the DMA1 for both single particles and multiple charged large particles, with a difference of ~1% (Figure 5B). the size of singly charged aerosol particles (200-350 nm, black circles in Fig.5B) were within the detection limit of SP2 scattering signal, but some double or triple charged aerosol particles (red circles in Fig.5B) was larger than the upper sizing limit of SP2 scattering signal (~400 nm). Figure 5B shows that the optical size of double charged or triple charged thick-coating BC particles agreed well with their theoretically calculated mobility diameter (323, 414, 438 and 508 nm). The agreement implies that the assumption on a spherical particle in Mie model calculation can be used for the thick-coated BC particles in our case. It also revealed that the LEO-fit method was applicable for ambient thick-coated BC particles under polluted conditions in China."
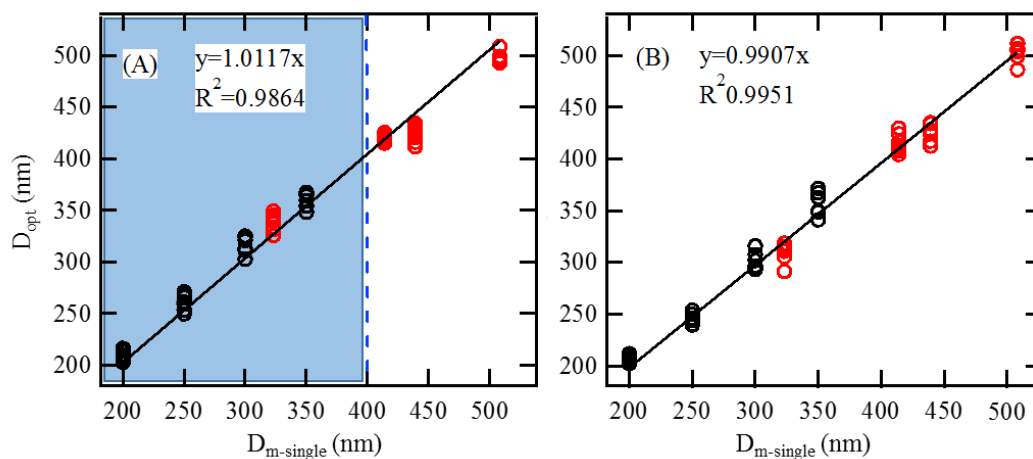
Fig. R3. (Figure 5 in the revised manuscript) Comparison of the mobility particle size as if they have only single charge ($D_{\text{m-single}}$) and their optical size (D_{opt}) derived from LEO-fit and Mie calculation for non-BC particles (A) and thick-coated BC particles (B). The black circles and red circles represent the single charged particle samples and double/triple charged particle samples, respectively. The blue dash line represents the upper limit of SP2 scattering detection (~400 nm). The light blue shade area represents the sizes range within SP2 sizing detection limit for purely scattering particles (i.e., non-BC particles).

.

6) *I find the authors' terminology regarding "non-BC", "internally-mixed BC" and "externally-mixed BC" confusing. There are non-BC and BC-containing particles. For BC-containing particles, there is then a distribution of relative coated amounts, with some particles having little coated (which I think the authors take to mean "externally mixed") and some having a lot of coated (here, I think, "internally mixed"). The authors make their definition based on a "lag-time" analysis. But, the validity of such a binary framework has not been justified here. Do they find a bimodal distribution of lagtimes, thus justifying the binary framework?*

Response: Thanks and yes, we did find a bimodal distribution of lagtime (Fig. R4). Here we adopted a classification method based on a threshold lag-time/coated

thickness) which is commonly used previous studies (e.g., Schwarz et al., 2006; Sedlacek et al., 2012; Subramanian et al., 2010). In literature, the two peaks were always observed and considered as the thin-coated or bare (externally-mixed) BC and thick-coated (internally-mixed) BC, respectively.

We include the Figure R4 about the distribution of lagtime in our SP2 measurements as Figure S1 in supplementary information. We have clarified the terminology about 'non-BC particles', 'BC-containing particles' and the sub categories of ' thin-coated or bare (externally mixed) BC' and ' thick-coated (internally-mixed) BC' in the revised manuscript: "*In this study, ambient particles are classified into non-BC particles and BC-containing particles. Particles with detectable amounts of rBC by SP2 are considered as BC-containing particles, and others are taken as non-BC particles. As shown in Fig. S1, the lagtime (Δt), namely the time difference between the occurrences of the peak of the incandescence and scattering signals measured by SP2 (Moteki and Kondo, 2007; Schwarz et al., 2006; Sedlacek et al., 2012; Subramanian et al., 2010), exhibits a clear two-mode distribution. Accordingly, we further classified the BC-containing particles into thin-coated (or bare) BC (Δt <1.6 μs) and thick-coated BC (Δt >=1.6 μs).*"
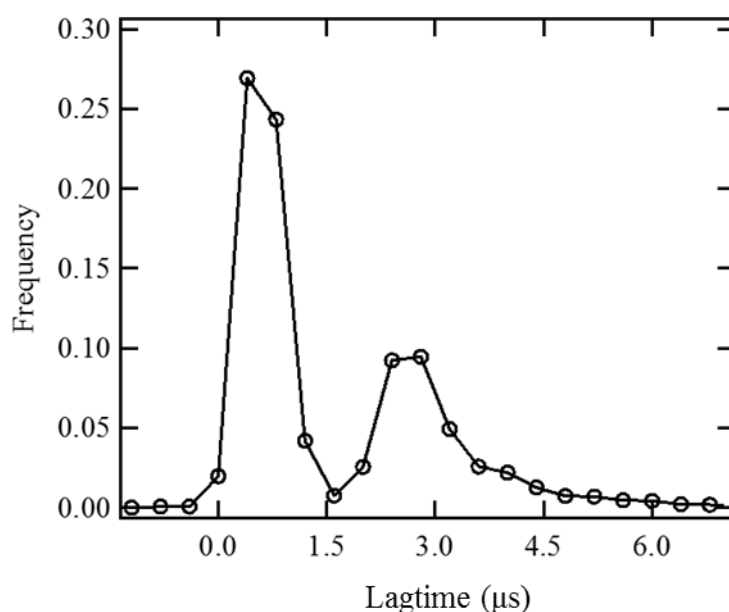
Fig. R4. (Figure S1 in the revised manuscript) The distribution of lagtime in our SP2

measurement.

(7) Fig. 4 and Discussion: The authors assume that BC is the only component of the particles when making their fractal dimension determination. This is an assumption that must be demonstrated in some way. What if, for example, there were a 10 nm thick "coated" on the "externally mixed" BC particles? This might still have a small lag time. But, depending on the particle size, the mass contribution could be substantial (e.g. for a 100 nm BC core, a 10 nm coated corresponds to nearly 40% of the mass, assuming equal densities and spheres.) How do the authors know that the only component contributing substantially to the particle mass is BC for these particles with small lag times? What sort of uncertainty is contributed by their assumption.

Response: This is a very good point. As the reviewer pointing out, a thin coated on the "externally mixed" BC may cause a large bias in the calculated effective density since particle mass is proportional to D_p^3. However, the effective density was only used to calculate the mobility diameter of thin-coated or bare (externally-mixed) BC particles from BC mass measured with SP2. The calculated mobility diameter of BC is with lower bias because diameter is proportional to ρ^{-3}. Taken a 200 nm particle as an example (the smallest size that we selected), assuming a maximum 20 nm thin coated (e.g., as in Subramanian et al., 2010), the bias of the mobility diameter of thin-coated or bare (externally-mixed) BC particles would be ~20%.

We have added a caveat in the related discussion and point out the possible error/uncertainties due to the possible thin coated on the externally mixed BC, as "*It should be noted that the presence of a thin coating can introduce biases in retrieving the mobility diameter of the thin-coated (or bare) BC particle by using the retrieved effective densities in Fig.4. Considering a maximum 20 nm thin coating (e.g., as in Subramanian et al., 2010), the uncertainty of the mobility diameter (200-350 nm) of a thin-coating (or bare) BC particle could be ~10-20%.*"

(8) P6/L19: The authors state: "For externally-mixed BC particles, a diameter is hard

to define due to their irregular morphology." This is not correct. A volume-equivalent or mass-equivalent diameter can be easily defined if the BC mass is measured and it is assumed that the particle is 100% BC (which the authors do here).

Response: Thanks. Here we meant to say "geometric diameter". The sentence has been revised, as "*For the thin-coated (or bare) BC particles, a geometric diameter is hard to define due to their irregular morphology (Park et al., 2003; Slowik et al., 2004).*"

(9) I find Fig. 5 unclear. For the mobility distributions (dN/dlogDp vs Dpm), is this from the measurements with the 2nd DMA? This is not stated. If so, why are the peaks so broad? The size distributions presented suggest that the authors were operating the first DMA with a very low resolution. Is that the case? If so, that would meant that the authors passed through particles with a broad distribution of actual mobility diameters.

Response: Thanks. Figure 5 (in the manuscript) shows the volume-equivalent and mobility diameter distribution of externally-mixed (thin-coated or bare) BC from SP2 measurements, not from the DMA2. The volume-equivalent diameter distributions were calculated from BC mass and BC material density (1.8 g/cm^3), while the mobility diameter distributions were calculated from BC mass and BC effective density shown in Fig. 4. To make it clear, we revised the caption of Figure 5 (Figure S3 in the revised manuscript) as "*The mass equivalent diameter ($D_{me,SP2}$) and mobility diameter ($D_{m,SP2}$) distribution from SP2 measurement for size-resolved thin-coated (or bare) BC at (A) 200 nm , (B) 250 nm (B), (C) 300 nm and (D) 350 nm. In SP2 calculation, the $D_{me,SP2}$ of a single BC particle was calculated from BC mass and BC material density (1.8 $g\ cm^{-3}$), while the $D_{m,SP2}$ of a single BC particle was calculated from BC mass and the predefined effective density shown in Fig. 4.*"
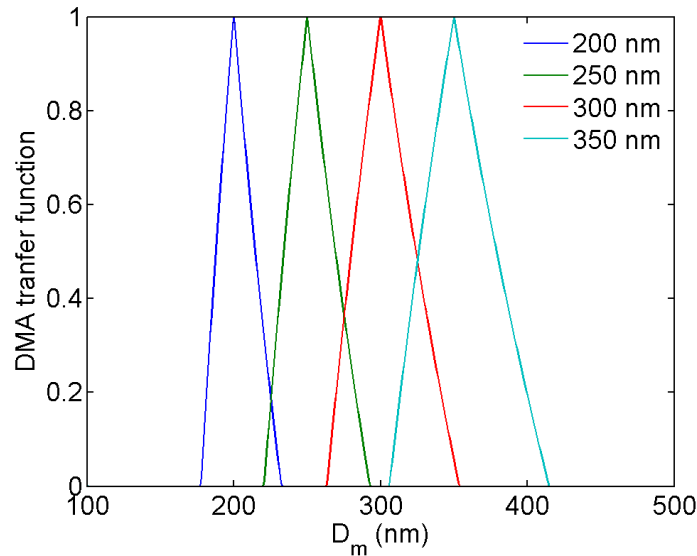
Fig. R5. The theoretical DMA transfer functions at an aerosol to sheath flow ratio of 1:5.

We were not operating the DMA1 with a low resolution. The aerosol to sheath flow ratio of the DMA1 is 1:5. Figure R5 shows the theoretical DMA transfer functions at this flow ratio. They are much narrower than the mobility distributions shown in Fig. 5 (red lines). The broadening effect caused by DMA transfer function is therefore limited. The broadening of the mobility distributions after the DMA1 is due to the use of a fixed effective density for externally-mixed (thin-coated or bare) BC particles when calculating their mobility diameter. Mobility diameter of particles with a certain mass/volume strongly depends on their morphology (quantified as dynamic shape factor). Since externally mixed BC particles are fractal-like agglomerates with varies shape factors (Zhang et al., 2008; Park et al., 2003; Pagels et al., 2009), particles output by the DMA with same or similar mobility may have a large range of mass, meaning also a large range of effective density. However, a fixed effective density was used for deriving the mobility diameters, which caused the broadening effect. We also note here that in each distribution in Fig. 5 (in the manuscript), the second smaller peak on the right side is due to the double charged particles.

(10) P7, L3: The authors' statements regarding the density of the BC are wrong. The

material density is 1.8 g/cm^3 (not 1.8 g/m^3, as stated). The conversion of the measured mass to a diameter requires specification of what diameter one is considering. One should absolutely use the material density if converting mass to a volume-equivalent diameter. To use a lower effective density is not correct. But, if the authors are aiming to estimate a mobility diameter from the mass, then the use of an effective density is appropriate. But, it is entirely unnecessary here since the argument is circular: the effective density is determined by comparing the selected mobility diameter with the observed volume equivalent diameter. So, conversion of the mass back to a mobility diameter is just a statement of the obvious.

Response: Thanks for the comment. We apologize for the typo, and we have changed the "1.8 g m^{-3}" into "*1.8 g cm^{-3}*".

We agree with the reviewer that the conversion of the measured mass to a diameter requires specification of what diameter one is considering. The reasons of showing the mobility diameter distribution are to have a direct comparison with the volume-equivalent diameter.

Following the review's suggestion, we have made following changes in the manuscript: "*The effective density of the thin-coated (or bare) BC particles at 200-350 nm observed at the Xianghe Site was found to be very small, ranging from 0.25 to 0.45 g cm^{-3}. It is significantly lower than the material density of carbon, ~1.8 g cm^{-3} (Metcalf et al., 2012; Schwarz et al., 2008; Subramanian et al., 2010). The large discrepancy between the effective density and material density of BC indicated that the thin-coated (or bare) BC particles measured at Xianghe was not a void-free structure. In order to compare with the sizing detection of VTMDA, we calculated the equivalent mobility diameter of the thin-coated (or bare) BC particles by dividing the rBC mass detected by SP2 by the effective density, which is significantly larger than the one calculated with the material density of carbon (see Fig. S3).*"

(11) P7,L9: A tandem DMA is also able to "separate aerosol particles with different

charges" if the particle stream is reneutralized. The DMA + SP2 is not unique in this regard.

Response: Thanks to the reviewer to point this out. We do not intent to claim that our approach is the only solution. We have deleted it in the revised manuscript.

(12) Fig. 6b: I find this to be unclear. Why are there so many points on the graph? There is a fixed ratio between the number of singly and doubly charged particles for each mobility diameter. Thus, there should be one point per size, as is indicated by the text on P7.

Response: Thanks. The different points in Fig. 6B (Figure S4B in the revised manuscript) represent samples observed at different days, while the distributions shown in Fig. 6A (Figure S4A in the revised manuscript) are the campaign averages. Due to variation of particle number size distribution on different days, the ratio between the number concentrations of single and double charged particles with same mobility is not fixed, resulting in different $R_{single-to-double}$ in Fig. 6B (Figure S4B in the revised manuscript).

To make this point clear, we have added "*The size distributions in (A) represents the campaign averages; the different points in the (B) represents samples observed at different days. Due to variation of particle number size distribution at different days, the ratio between the number concentrations of singly and doubly charged particles with same mobility is not fixed, resulting in different $R_{single-to-double}$.*" in the caption of Figure 6 (Figure S4 in the revised manuscript).

(13) P7/L29: Again, the authors refer to the accuracy of their size determination. But, they have forced agreement. Thus, this is simply a statement that the authors have calibrated their instrument.

Response: Thanks. The main purpose of displaying Fig. 6B (Figure S4B in the

revised manuscript) is to further explore the possibility of using LEO-fit method to extend its sizing ability towards larger size range. To make this point clear, we have removed "Our results further revealed that the accurate particle size was derived by our method (discussed in Sect. 3.3.1 and Sect. 3.3.2) based on SP2 measurement." in the revised manuscript, and have added "*which supported that the LEO-fit for larger particles with saturated scattering signals was valid.*"

(14) Fig. 7: The authors show the SP2 distribution as a sum over different particle types. However, this does not take into account the important issue that the SP2 instrument detection limit is different for scattering and incandescence. The SP2 cannot measure scattering by particles below some size. But this is not the same size below which it cannot measure incandescence. Ultimately, one cannot simply add up the size distributions from the different types of particles from the SP2 without accounting for such effects as it can give a misleading picture.

Response: The SP2 data used in Fig. 7 in the manuscript is based on only incandescence measurements and the different instrument detection limit is not an issue here.

To clarify it, when discussing the Fig. 7 (Figure 9 in the revised manuscript), we have added "*Note that the SP2 detection efficiency (Fig. S9) and experimentally determined effective density (1.2 g cm^{-3} for BC cores of thick-coated BC and 0.25-0.45 g cm^{-3} for thin-coated (or bare) BC) have been considered in the calculation of the rBC size distribution.*

As shown in Fig. 9, the mobility size distribution of rBC measured by SP2 was significantly different with that of the refractory residues at 300 ℃ measured by VTDMA……Above the incandescence detection limit of SP2 (BC particles with diameter larger than ~70 nm), ……"

(15) Fig. 7 and Fig. S2: The authors need to refer to their diameters using some sort of specific terminology. They are not "rBC diameters." They are, perhaps

"mobilityequivalent diameters". The authors must be precise in their terminology. As it is, the lack of precision makes the concepts presented difficult to follow.

Response: Thanks for the suggestion. We have changed "rBC size" into "*Mobility size distributions of BC cores*".

(16) P8,L15: It is entirely unclear in what way specifically the "VTDMA measurement had a large uncertainty." What is meant by "uncertainty" here? The VTDMA measurement is what it is. Also, the authors have not demonstrated an ability to measure what are predominately mostly scattering particles below 200 nm: their entire validation exercise used particles with mobility diameters >= 200 nm. It is not surprising that the SP2 does not measure as many purely scattering particles at smaller sizes compared to the VTDMA as it is not designed to do so. What the authors need to show is an efficiency curve, similar to that shown for BC in Fig. S1, but for scattering-only particles. Below what size does the detection efficiency fall off for scattering only particles? Also, it is unclear what the authors mean by a "significant different in BC mixing state" Between the measurements. Different in what way? What is being determined?

Response: Thanks to the reviewer for raising this concern. VTDMA was designed to measure the refractory residues at certain temperatures. In previous VTDMA-based studies, refractory residues larger than 50 nm at 300 ℃ were usually considered as BC (Philippin et al., 2004; Wehner et al., 2009; and Cheng et al., 2009). In Fig. 7 (Figure 9 in the revised manuscript), the discrepancy between the number size distributions of refractory residues and BC cores for diameter larger than 70 nm indicates that at Xianghe site a large fraction of the refractory residuals at 300 ℃ are not BC, suggesting that the assumption made in previous VTDMA studies that most of refractory residuals at 300 ℃ were BC may need to be reconsidered.

To the second question, since we discussed only the distribution of BC cores determined by incandescence signal in SP2. The detection limit of scattering signal did not play a role here. Still, we provide the detection efficiency curve of pure

scattering particles for our SP2 here in Figure R6.

To the last question, SP2 gives the mixing state of BC, while VTDMA gives the mixing state of refractory material. They are comparable only if assuming the refractory material at 300 ℃ is BC. But as discussed above, this seems not the case in our study.
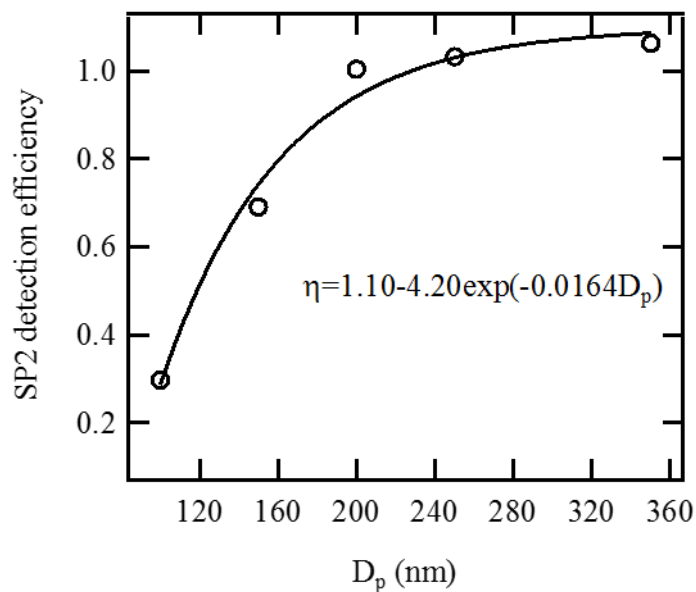
Fig. R6. The SP2 detection efficiencies (η) for non-BC particles at different size (100-350 nm).

We agree with the reviewer that the statement "VTDMA measurement had a large uncertainty" may be misleading here. We have clarified it by rewriting P8/L8-25 as: "*As shown in Fig.9, the mobility size distribution of rBC measured by SP2 was significantly different with that of the refractory residues at 300 ℃ measured by VTDMA. The SP2 measured one shows two peaks, one at around the prescribed size (200, 250, 300 and 350 nm selected by DMA1) and another one at a smaller size, representing the thin-coating BC (or bare BC) and thick-coating BC particles, respectively. For VTDMA measurement, the number size distribution of low-volatile residues at 300 ℃ also shows a peak at the prescribed size, and other two peaks at smaller sizes, which is similar to the previous measurements in Beijing (Cheng et al.,*

2012). Above the detection limit of SP2 incandescence (BC particles with larger than ~70 nm), the number concentration of BC particles measured by SP2 accounted for only 16-35% of the residual particles measured by VTDMA. This large discrepancy indicated a large fraction of non-BC low-volatile components, which could not completely evaporate at 300 ℃ exists in the aerosol particles at Xianghe site, such as low volatile organic matter, refractory mineral dust, trace metals and sea salt (Cheng et al., 2009; Ehn et al., 2014; Kalberer et al., 2004). Furthermore, we found that most of the non-shrinking refractory residues (~78-91%) (the 1st peak of the DMA2) are detected as rBC particles by SP2, while there are about 80-90% of the residues larger than ~70 nm in the other two peaks (the 2nd and 3rd peaks) of the DMA2 (shrank particles) are not rBC, as they did not show incandescence signal in SP2. In previous studies involving thermodenuder technique, it has often been assumed that the refractory residual materials at 250 to 400 ℃ were BC components (Philippin et al., 2004; Wehner et al., 2009; and Cheng et al., 2009; Cappa et al., 2012; Liu et al., 2015; Liu et al. 2017). But, this assumption may not hold at the sub-urban site of Beijing (Xianghe), and may cause a significant overestimation of the number of internally mixed BC particles. On the other hand, this assumption may leads to the underestimation of the light absorption enhancement factors in the North China Plain due to the remaining low-volatile non-BC materials coating on the BC particles after heated by the thermodenuder."
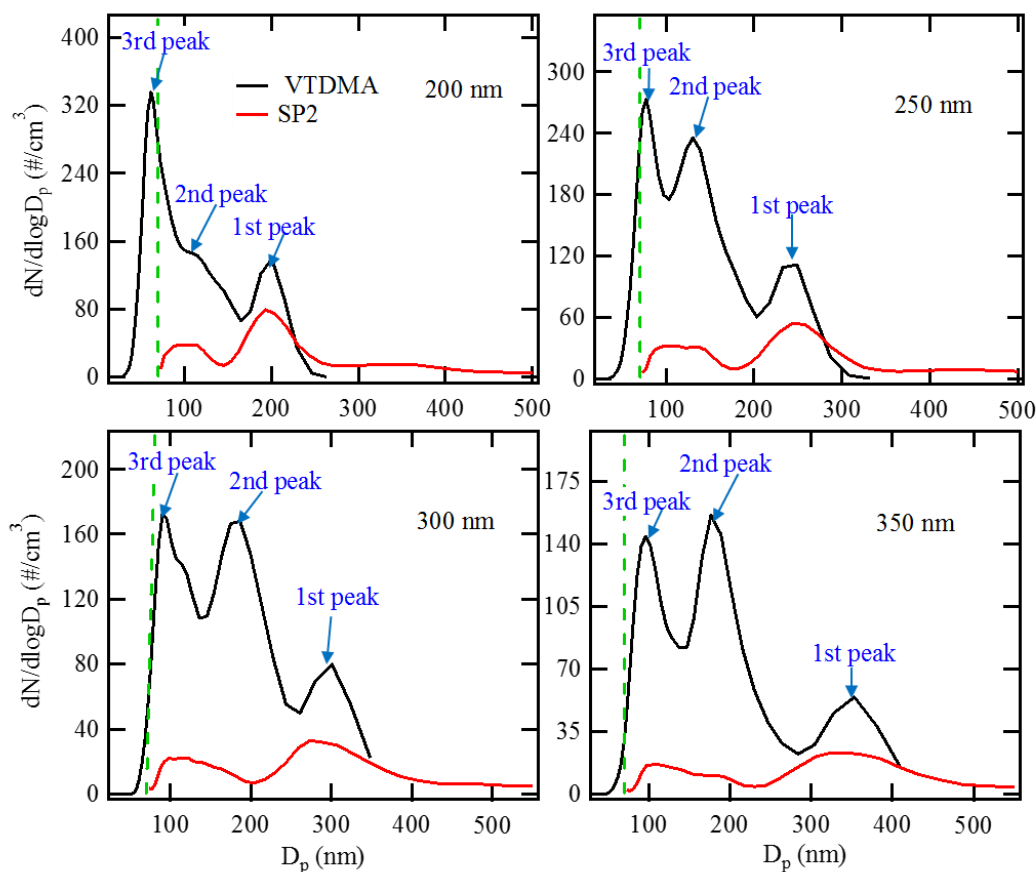
Fig. R7. (Figure 9 in the revised manuscript) Mobility size distributions of the refractory BC measured by SP2 (red lines) and that of the residual materials from VTDMA measurement at 300 ℃ (black lines). The green dash line represents the lower limit of SP2 incandescence detection (~70 nm). The initial particle sizes selected by DMA1 were 200, 250, 300 and 350 nm.

 (17) P8/L14-25: I find this paragraph very difficult to understand. The SP2 cannot measure small particles. I do not see how comparing the SP2 to the VTDMA in this particular way is addressing limitations of the VTDMA.

Response: Thanks to the reviewer to raise this concern. Sorry for the misleading and we are not aiming to addressing the limitation of VTDMA. Here, we only compare the number size distribution of refractory residues measured by the DMA2 of VTDMA and the BC particles detected by SP2 above its incandescence detection limit (>70 nm BC particles). The number size distribution of BC cores from SP2

measurement (red lines in Figure 7 in the manuscript) is corrected for SP2 incandesce particle-counting efficiency according to calibration curve (Figure R8 in response). Therefore, the detection limit of scattering signal is not an issue here.
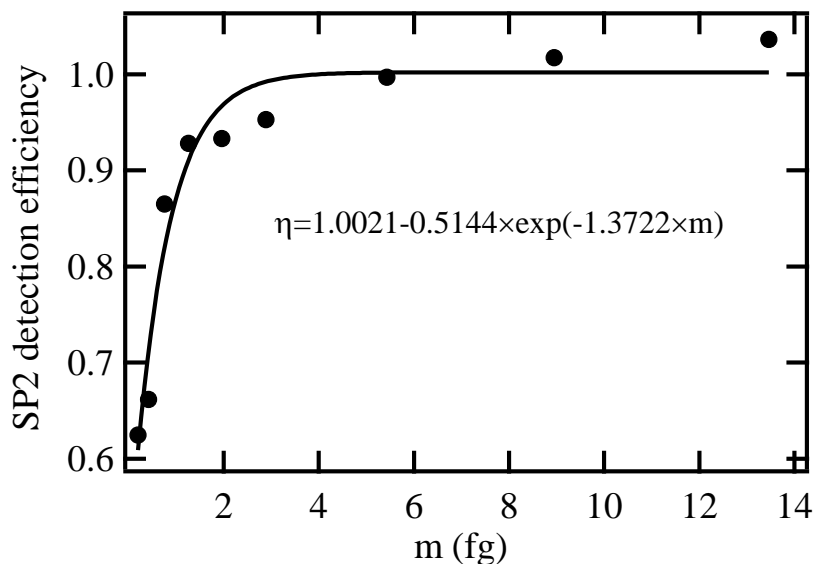
Fig. R8 (Figure S9 in the revised manuscript). The SP2 detection efficiencies (η) in each BC mass-bin.

The last two paragraphs in Sect. 3.2 have been rewritten according to the two comments above (see the above response).

(18) Fig. 7 vs. Fig. 8: Considering the authors' own measurements, there is an inconsistency between these two figures. The SP2 size distributions shown in Fig. 7 suggest that the distribution is dominated by "externally-mixed BC" particles. But, Fig. 8 clearly indicates that the number is dominated by "non-BC" particles. Fig. 8 is thus more consistent with the VTDMA measurements shown in Fig. 7, which shows a substantial fraction of what might be considered "non-BC" particles (i.e. the particles that shrank a lot). Yet, the authors just spent a section arguing that the SP2 does a better job than the VTDMA. These discussions must be aligned and reconciled..

Response: Thanks to the reviewer. There might be some misunderstanding. In Fig. 7 in the manuscript, we discussed about BC-containing particles (internally-mixed

(thick-coated) BC and externally-mixed (thin-coated or bare) BC particles). But, Fig. 8A in the manuscript shows the number fractions of all particles (i.e., non-BC, internally-mixed (thick-coated) BC and externally-mixed (thin-coated or bare) BC particles).

To make it clear, we revised the caption of Figure 8 (Figure 6 in the revised manuscript) as "*Number (A) and mass (B) composition of ambient particle samples (non-BC, thin-coated (or bare) BC and thick-coated BC) with different mobility diameters (200, 250, 300 and 350 nm).*"

(19) P9,L6: It is unclear how a small BC fraction necessarily indicates "long range transport." This must be justified. Yes, it suggests that there is secondary processing (most likely), but why "long range transport" specifically? The authors seem to take this as a given. Why not local photochemical or nocturnal processing?

Response: Thanks for the comment. We agree with the reviewer that the aging of BC particles may not need to experience the long-range transport. BC is primary aerosol component emitted during combustion process (biomass and fossil fuel burning). BC aging degree (i.e., coated thickness and D_p/D_c ratio) in the atmosphere strongly depends on secondary processing (Metcalf et al., 2013). The more secondary aerosols (i.e., non-BC species such as SOA, sulfate and nitrate) formed in the atmosphere the higher BC aging degree and thicker coated. BC aging process may occur locally or during regional transport. In this study, we cannot distinguish between them.

We have changed "long range transport" into "*secondary process*" and in manuscript it reads as "*revealed that the aerosol particles sampled at our site were likely undergone a strong secondary aging process.*"

(20) P9/L11: The authors state here that the fraction of internally-mixed particles at 200-300 nm was 38-51%. But, above, they say that these particles are only 7-10%, including externally-mixed particles. Clearly there is a discrepancy. Fig. 8 and Fig. 9

are similarly inconsistent. Perhaps they are talking about only the BC-containing particles. But this is unclear.

Response: Thanks. In Fig. 8 in the manuscript, we talked about all particles, including non-BC, thick-coated (internally-mixed) BC and thin-coated or bare (externally-mixed) BC particles. In Fig. 9 in the manuscript, we talked about only the BC-containing particles.

To make it clear, we have changed the "the fraction of internally-mixed particles" in P9/L11 into "*the fraction of thick-coated BC particles in total BC-containing particles (F_{In-BC})*".

(21) P9/L13: How do the authors know that the peak is from both photochemical formation and regional transport? How is the influence of regional transport identified? Why not just local production?

Response: Thanks. As responded to comment (19), we have changed "The peak around noontime can be attributed to secondary photochemical formation and regional transport" into "*The peak around noontime and early afternoon can be attributed to photochemical aging (Cheng et al., 2012)*"

(22) P9/L16: The authors compare their current results to those of Cheng et al. for Beijing. They should note that Cheng et al. also made measurements in Beijing.

Response: Thanks for the suggestion. The sentence has been revised as "*which was consistent with the finding of Cheng et al. (2012) at another site around urban area of Beijing (~60 km from Xianghe site).*"

(23) Fig. 10: Much more meaningful would be a histogram of the Dp/Dc values. The justification for binning as was done here is not clear.

Response: Following reviewer's suggestion, we have changed the Fig. 10 in the manuscript into a histogram. As shown below (Figure R9 in response):
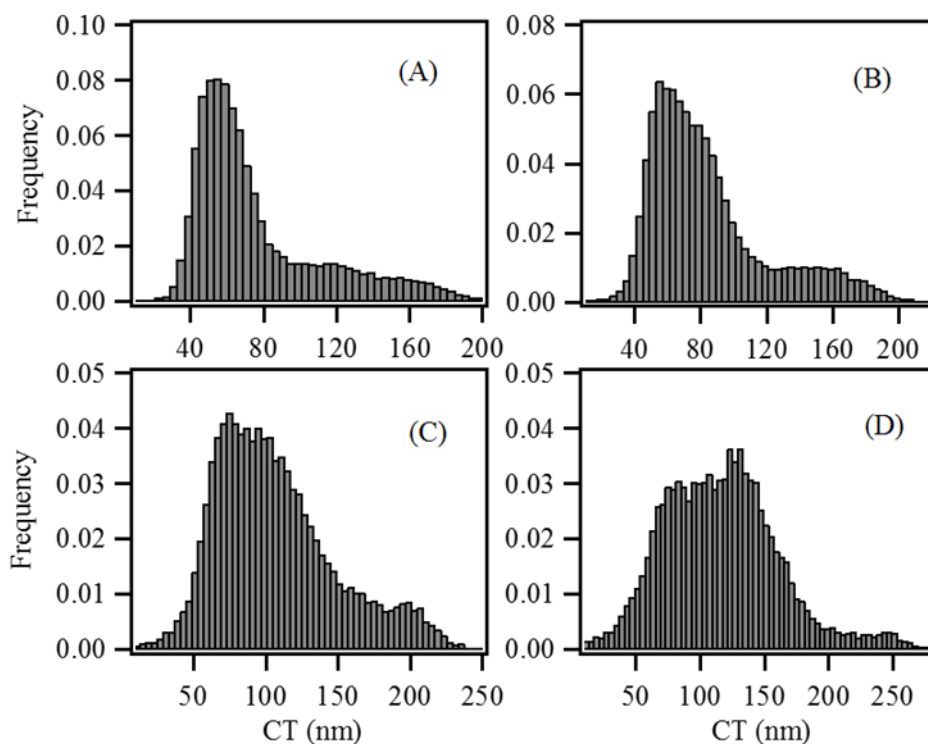
Figure. R9. (Figure 8 in the revised manuscript) Frequency distribution of coating thickness (*CT*) for the thick-coated BC particles at different mobility diameters, 200 (A), 250 (B), 300 (C) and 350 nm (D).

Correspondingly, we also revised the discussion on Figure 10 (Figure 8 in the revised manuscript): "*Figure 8 shows frequency distribution of coating thickness (CT) for the thick-coated BC particles at 200-350 nm. The observed thick-coated BC particles are dominated by particles with CT of 40-200 nm and the core diameters of thick-coating particles have a narrow distribution with mode centers located at 100-150 nm (Fig. S6). Since BC is primary aerosol component and cannot be produced secondarily, larger particles usually have thicker coatings. We found that the aging degree of the thick-coated BC particles increased as the particle size increases (Fig. S7), e.g., the average CT of thick-coated BC particles at 200, 250, 300 and 350 nm were respectively 74, 80, 100 and 108 nm.*"

(24) P9/L20: It is not at all surprising that the "internally-mixed" particles have thick coateds. This is by definition, as the authors have discriminated by the difference in lag times and thus we would fully expect that the particles should have large Dp/Dc ratios. If they did not, they would not have been identified as "internally mixed" in the first place. What is the relationship between lag time and Dp/Dc for this study? How are the authors skewing their analysis by deciding on a particular lag time cutoff.

Response: Thanks to the reviewer. The lagtime method is commonly used in previous SP2 studies (e.g., Schwarz et al., 2006; Sedlacek et al., 2012; Subramanian et al., 2010). We know it might not be the perfect way, but currently it is the only way to get the mobility diameter distribution of both thin-coated or bare (externally-mixed) BC and BC cores in thick-coated (internally-mixed) BC particles from SP2 measurement. The reason is that we cannot retrieve the optical diameters of thin-coated or bare (externally-mixed) BC with Mie model is because they may have irregular shapes (Figure 4 in the manuscript). This is also a limitation of SP2 technique. There is no simple relation between lag time and D_p/D_c, since the lag time also depends on the location of BC core in particles.

By "thick coated" and "strongly enhanced absorption", we didn't mean to compare with thin-coated or bare (externally mixed) BC, but to compare with results at other less polluted locations. The bimodal distribution of lagtime is commonly observed, e.g., in Long Island site (Sedlacek et al., 2012), Mexico site (Subramanian et al., 2010), where the coated thickness (~30-60 nm) of thick-coated (internally-mixed) BC is thinner than that of our study.

To make it clear, we added "*In this work, we found that the thick-coated BC particles observed in North China Plain showed a significantly larger CT (74-108 nm) than that at other less polluted locations (CT of ~30 to ~60 nm), e.g., Long Island (NY, USA) in summer time (Sedlacek et al., 2012), Mexico City in spring time (Subramanian et al., 2010), Fukue Island (Japan) in spring time (Shiraiwa et al., 2008) and Weybourne (UK) in summer time (Liu et al., 2013). The results revealed that BC at our observation site was more aged, which can be attributed to stronger*

secondary processes in the atmosphere (e.g., oxidation of SO₂, NOₓ and volatile organic carbon (VOC) to sulfate, nitrate and secondary organic aerosol (SOA), respectively) (Andreae et al., 2008; Zheng et al., 2015; Cheng et al., 2016)." in the manuscript.

(25) P9/L22: The authors should comment further on the observation that Dp/Dc increases as Dp increases. (They might even make a plot…). Why do they think this is the case? What physical insights can be discerned?

Response: As shown in Fig. R10, core diameters of BC-containing particles have a narrow distribution with mode centers located at 100-150 nm, since BC is primary aerosol component. Therefore, larger particles usually have also a thicker coated and larger D_p/D_c (Fig. R11), as a consequence of condensation and coagulation, which happen mostly between BC and non-BC species.

To make it clear, we revised the sentence as "*Figure 8 shows frequency distribution of coating thickness (CT) for the thick-coated BC particles at 200-350 nm. The observed thick-coated BC particles are dominated by particles with CT of 40-200 nm and the core diameters of thick-coating particles have a narrow distribution with mode centers located at 100-150 nm (Figure S6). Since BC is primary aerosol component and cannot be produced secondarily, larger particles usually have thicker coatings. We found that the aging degree of the thick-coated BC particles increased as the particle size increases (Fig. S7), e.g., the average CT of thick-coated BC particles at 200, 250, 300 and 350 nm were respectively 74, 80, 100 and 108 nm.* "
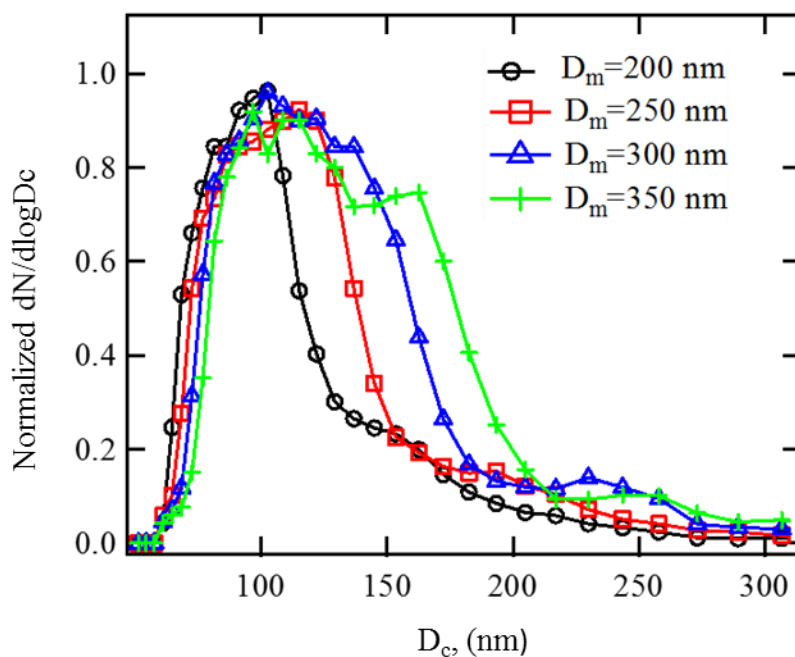
Fig. R10. (Figure S6 in the revised manuscript). The number size distribution of BC cores for thick-coated BC particles.
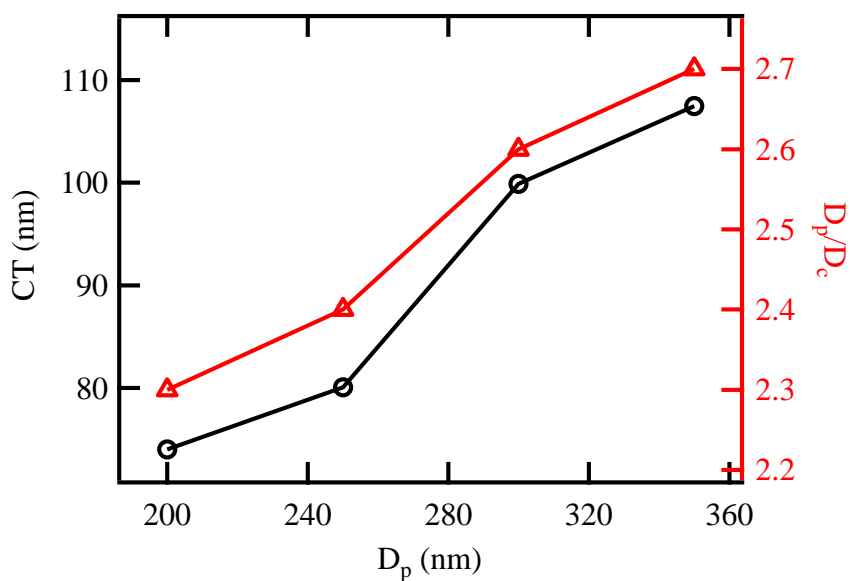
Fig. R11. (Figure S7 in the revised manuscript). The average *CT* and D_p/D_c ratio of thick-coated BC particles at different size (200-350 nm).

(26) P9/L22: The authors again point to long range transport. Why is local photochemical production of coateds not possible, especially given that there is clearly a local source of BC?

Response: Thanks for the comment. We agree that this statement is inappropriate. We have changed "long range transport" into "*secondary process*". See response to (19).

(27) P9/L27: The authors cite Zhang et al., (2016b) to support their statements regarding potential for absorption enhancement. But, (i) Zhang et al simply provide calculations that say that when BC particles are coated absorption can be enhanced, which has been known for a long time since before Zhang and (ii) the Zhang results are simply calculations, and the actual magnitude of absorption enhancements in the atmosphere remains unresolved. The authors should provide a fuller discussion and not simply self-cite.

Response: Thanks for the comment. We have deleted the sentence and added the following discussion in the manuscript, as shown below:

"Aged BC particles with thick coating under the polluted conditions in China may imply that the light absorption of the thick-coated BC particles observed in the North China Plain could be significantly enhanced by lensing effects (Fuller et al., 1999; Lack and Cappa, 2010; Liu et al., 2015; Moffet et al., 2009). Although, the actual magnitude of absorption enhancements of BC aerosol in the atmosphere remains unresolved due to complex morphology and inhomogeneity of ambient BC-containing particles (Adachi et al., 2013; Cappa et al., 2012; Fuller et al., 1999; He et al., 2015; Liu et al., 2015; Liu et al., 2017), the good agreement between LEO-fit retrieved optical particle diameter and mobility one for the thick-coated BC particles (Fig. 5(B)) suggested that the spherical core-shell assumption may be applicable in our case. Based on this assumption in the Mie simulation, the light absorption enhancement caused by the thick coatings on BC particles was ~1.8-2.1 during our campaign period."

(28) Fig. 11: This figure is fundamentally misleading. The SP2 cannot measure the size of particles via the optical method if they are too small. The lower-limit size differs for BC measurement vs. for size measurement. Thus, there is an intrinsic bias in the method that makes it appear as if the coated thicknesses of small BC particles

are larger, on average, than they might be. Consider a 100 nm core. If the smallest optical diameter that can be measured is 150 nm, then the thinnest coated is 25 nm. There is no information about the concentration of 100 nm cores with CT < 25 nm. It may be that the decrease in coated thickness with core size, shown in Fig. 11, is valid. But, the authors must demonstrate that their measurements are not biased by differences in the lower-limit size for BC vs. for optics.

Response: Thanks for the comment. The effect pointed out by the reviewer only exists when measuring poly-dispersed aerosol with SP2 (without a DMA upstream) due to a fraction of particles with size lower than SP2 detection limit. But in our study, we do not have such a problem since what we measured is mono-dispersed aerosol particles (pre-selected by the DMA1) with diameters higher than the scattering detect limit of SP2 (200, 250, 300, 350 nm vs. ~200 nm).

*(29) Fig. 11: The authors say that their curves follow "diffusion-controlled growth." But, looked at another way there is absolutely no reason to think that they would obtain any other result, given their method. They size select at a given size. And they measure a core size. By definition, Dselected = Dcore + 2*CT. Thus, there is a definite relationship between their coated thickness and Dcore. Further, the curves shown generally follow this curve. For a 100 nm core, the "coated thickness" for a 200, 250, 300 and 350 nm selected size is 50, 75, 100 and 125 nm. These are nearly identical to what the authors obtain. In other words, their graphs show exactly what is expected based on simple algebra, with no need to invoke "diffusion-controlled growth." Or, put another way, the results do not provide any information on the growth mechanism nor do they demonstrate that coated thicknesses decrease with core diameter. The entire discussion regarding Fig. 10 needs to be either removed or substantially revised. And if revised, needs to move beyond the simple algebraic expectation to provide some physical insight.*

Response: Thanks for the comment. We agree with the reviewer that we can not conclude "diffusion-controlled growth" from Fig. 11 (Fig. R12 in response). We have deleted the statement in the manuscript.

However, Fig. 11 (Fig. R12 in response) provides additional information on the relation between coated thicknesses and core size. For a certain core, the coated thickness in Fig. 11 shows a wide range rather than a value of $CT=(D_{selected}-D_{core})/2$, because the size of the particles selected by DMA still exhibited a distribution. Moreover, Figure 11 also shows the modes of coated thickness for the doubly and triply charged particles (black and gray dashed lines in Fig. R12).
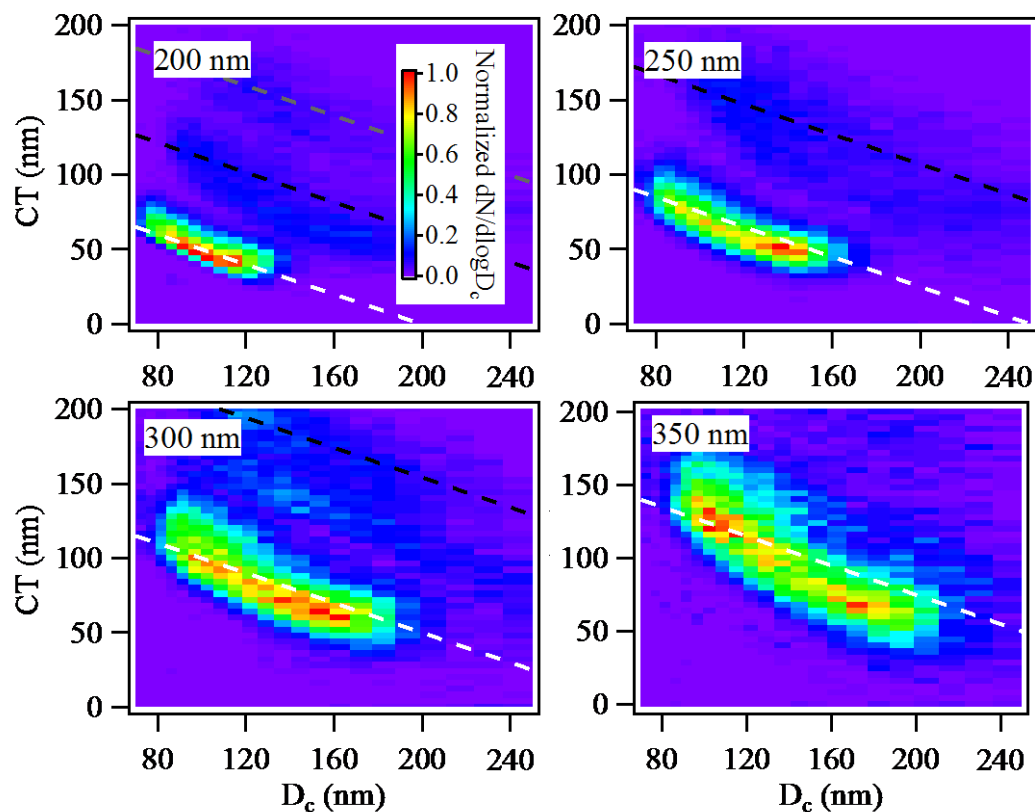
Fig. R12 (Figure S8 in the revised manuscript). Coated thickness (*CT*) of thick-coated BC particles at 200-350 nm (selected by DMA1) as a function of rBC core size (*Dc*). The dash line is $CT=(D_{selected}-D_c)/2$, i.e., the theoretic *CT*; the white, black and grey colors reflect the singly, doubly and triply charged particles.

Since Fig. 11 in the manuscript gives some information of the influence of DMA transfer function and multiple charged particles on the distribution of *CT*, we decided to move it to Supplement (Fig. S8). We have modified Fig. 11. The discussion on Fig. 11 (Figure S8 in the revised manuscript) have be revised in the manuscript "*Figure S8 shows the coating thickness of thick-coated BC particles as a function of rBC core*

size (D_c). For a certain core size, the coating thickness in Fig. S7 shows a wide distribution rather than a value of CT=($D_{selected}$-D_c)/2 (here, $D_{selected}$ is the mobility diameter selected by DMA1), because the size of the particles selected by DMA1 still exhibited a distribution determined by the DMA transfer function. For the single charged particles (white dashed lines in Fig. S8) at 200-350 nm, the D_c and CT showed a wide mode, which were in the range of ~80-200 nm and ~50-150 nm, respectively. Moreover, Figure S8 also shows the modes of coating thickness from the double and triple charged particles (black and gray dashed lines in Fig. S8). The wide range of D_c and CT revealed that the thick-coated BC particles at our site consisted of a mixture of BC from various sources of the North China Plain. The more coatings on BC the longer and/or faster secondary process the BC-containing particles underwent."

References:

Adachi, K., and Buseck, P. R.: Changes of ns-soot mixing states and shapes in an urban area during CalNex, *J. Geophys. Res.: Atmos.*, 118, 3723-3730, 2013.

Cappa, C. D., Onasch, T. B., Massoli, P., Worsnop, D. R., Bates, T. S., Cross, E. S., Davidovits, P., Hakala, J., Hayden, K. L., Jobson, B. T., Kolesar, K. R., Lack, D. A., Lerner, B. M., Li, S. M., Mellon, D., Nuaaman, I., Olfert, J. S., Petaja, T., Quinn, P. K., Song, C., Subramanian, R., Williams, E. J., and Zaveri, R. A.: Radiative Absorption Enhancements Due to the Mixing State of Atmospheric Black Carbon, *Science*, 337 (6098), 1078-1081, 2012.

Cheng, Y., Berghof, M., Garland, R. M., Wiedensohler, A., Wehner, B., Müller, T., Su, H., Zhang, Y., Achert, P., Nowak, A., Pöschl, U., Zhu, T., Hu, M., and Zeng, L.: Influence of soot mixing state on aerosol light absorption and single scattering albedo during air mass aging at a polluted regional site in northeastern China, *J. Geophys. Res.*, 114, (D10), D010883, 2009.

Cheng, Y. F., Su, H., Rose, D., Gunthe, S. S., Berghof, M., Wehner, B., Achtert, P., Nowak, A., Takegawa, N., Kondo, Y., Shiraiwa, M., Gong, Y. G., Shao, M., Hu, M., Zhu, T., Zhang, Y. H., Carmichael, G. R., Wiedensohler, A., Andreae, M. O., and

Pöschl, U.: Size-resolved measurement of the mixing state of soot in the megacity Beijing, China: diurnal cycle, aging and parameterization, *Atmos. Chem. Phys.*, 12, 4477-4491, 2012.

Ehn, M., Thornton, J. A., Kleist, E., Sipila, M., Junninen, H., Pullinen, I., Springer, M., Rubach, F., Tillmann, R., Lee, B., Lopez-Hilfiker, F., Andres, S., Acir, I.-H., Rissanen, M., Jokinen, T., Schobesberger, S., Kangasluoma, J., Kontkanen, J., Nieminen, T., Kurten, T., Nielsen, L. B., Jorgensen, S., Kjaergaard, H. G., Canagaratna, M., Maso, M. D., Berndt, T., Petaja, T., Wahner, A., Kerminen, V.-M., Kulmala, M., Worsnop, D. R., Wildt, J., and Mentel, T. F.: A large source of low-volatility secondary organic aerosol, *Nature*, 506, 476-479, 2014.

Fuller, K. A., Malm, W. C., and Kreidenweis, S. M.: Effects of mixing on extinction by carbonaceous particles, *J. Geophys. Res.-Atmos.*, 104, 15941-15954, 1999.

Gao, R. S., Schwarz, J. P., Kelly, K. K., Fahey, D. W., Watts, L. A., Thompson, T. L., Spackman, J. R., Slowik, J. G., Cross, E. S., Han, J. H., Davidovits, P., Onasch, T. B., and Worsnop, D. R.: A Novel Method for Estimating Light-Scattering Properties of Soot Aerosols Using a Modified Single-Particle Soot Photometer, *Aerosol Sci. Technol.*, 41, 125-135, 2007.

Hänel, G.: The real part of the mean complex refractive index and the mean density of samples of atmospheric aerosol particles, *Tellus*, 20, 371-379, 1968.

He, C., Liou, K. N., Takano, Y., Zhang, R., Levy Zamora, M., Yang, P., Li, Q., and Leung, L. R.: Variation of the radiative properties during black carbon aging: theoretical and experimental intercomparison, *Atmos. Chem. Phys.*, 15, 11967-11980, 2015.

Kalberer, M., Paulsen, D., Sax, M., Steinbacher, M., Dommen, J., Prevot, A. S. H., Fisseha, R., Weingartner, E., Frankevich, V., Zenobi, R., and Baltensperger, U.: Identification of Polymers as Major Components of Atmospheric Organic Aerosols, *Science*, 303, 1659-1662, 2004.

Lack, D. A. and Cappa, C. D.: Impact of brown and clear carbon on light absorption enhancement, single scatter albedo and absorption wavelength dependence of black carbon, *Atmos. Chem. Phys.*, 10, 4207–4220, 2010.

Liu, D., Whitehead, J., Alfarra, M. R., Reyes-Villegas, E., Spracklen, D. V.,

Reddington, C. L., Kong, S., Williams, P. I., Ting, Y.-C., Haslett, S., Taylor, J. W., Flynn, M. J., Morgan, W. T., McFiggans, G., Coe, H., and Allan, J. D.: Black-carbon absorption enhancement in the atmosphere determined by particle mixing state, *Nature Geosci*, 10, 184-188, 2017.

Liu, S., Aiken, A. C., Gorkowski, K., Dubey, M. K., Cappa, C. D., Williams, L. R., Herndon, S. C., Massoli, P., Fortner, E. C., Chhabra, P. S., Brooks, W. A., Onasch, T. B., Jayne, J. T., Worsnop, D. R., China, S., Sharma, N., Mazzoleni, C., Xu, L., Ng, N. L., Liu, D., Allan, J. D., Lee, J. D., Fleming, Z. L., Mohr, C., Zotter, P., Szidat, S., and Prévôt, A. S. H.: Enhanced light absorption by mixed source black and brown carbon particles in UK winter, *Nat Commun*., 6, 8435, 2015.

Marley, N. A., Gaffney, J. S., Baird, J. C., Blazer, C. A., Drayton, P. J., and Frederick, J. E.: An Empirical Method for the Determination of the Complex Refractive Index of Size-Fractionated Atmospheric Aerosols for Radiative Transfer Calculations, *Aerosol Sci. Technol.*, 34, 535-549, 2001.

Metcalf, A. R., Craven, J. S., Ensberg, J. J., Brioude, J., Angevine, W., Sorooshian, A., Duong, H. T., Jonsson, H. H., Flagan, R. C., and Seinfeld, J. H.: Black carbon aerosol over the Los Angeles Basin during CalNex, *J. Geophys. Res.-Atmos.*, 117, 2012.

Moffet, R. C. and Prather, K. A.: In-situ measurements of the mixing state and optical properties of soot with implications for radiative forcing estimates, P. Natl. Acad. Sci. USA, 106, 11872–11877, 2009.

Pagels, J., Khalizov, A. F., McMurry, P. H., and Zhang, R. Y.: Processing of Soot by Controlled Sulphuric Acid and Water Condensation Mass and Mobility Relationship, Aerosol Sci. Technol., 43 (7), 629-640, 2009.

Park, K., Cao, F., Kittelson, D. B., and McMurry, P. H.: Relationship between particle mass and mobility for diesel exhaust particles, Environ. Sci. Technol., 37 (3), 577-583, 2003.

Philippin, S., Wiedensohler , A., and Stratmann, F.: Measurements of non-volatile fractions of pollution aerosols with an eight-tube volatility tandem differential mobility analyzer (VTDMA-8), *Aerosol Sci.*, 35, 185-203, 2004.

Schkolnik, G., Chand, D., Hoffer, A., Andreae, M. O., Erlick, C., Swietlicki, E., and Rudich, Y.: Constraining the density and complex refractive index of elemental and

organic carbon in biomass burning aerosol using optical and chemical measurements, *Atmos. Environ.*, 41, 1107-1118, 2007.

Schwarz, J. P., Gao, R. S., Spackman, J. R., Watts, L. A., Thomson, D. S., Fahey, D. W., Ryerson, T. B., Peischl, J., Holloway, J. S., Trainer, M., Frost, G. J., Baynard, T., Lack, D. A., de Gouw, J. A., Warneke, C., and Del Negro, L. A.: Measurement of the mixing state, mass, and optical size of individual black carbon particles in urban and biomass burning emissions, *Geophys. Res. Lett.*, 35, 2008.

Schwarz, J. P., Gao, R. S., Fahey, D. W., Thomson, D. S., Watts, L. A., Wilson, J. C., Reeves, J. M., Darbeheshti, M., Baumgardner, D. G., Kok, G. L., Chung, S. H., Schulz, M., Hendricks, J., Lauer, A., Kärcher, B., Slowik, J. G., Rosenlof, K. H., Thompson, T. L., Langford, A. O., Loewenstein, M., and Aikin, K. C.: Single-Particle Measurements of Midlatitude Black Carbon and Light-Scattering Aerosols from the Boundary Layer to the Lower Stratosphere, *J. Geophys. Res.: Atmos.*, 111 (D16), D16207, 2006.

Sedlacek, A. J., Lewis, E. R., Kleinman, L., Xu, J., and Zhang, Q.: Determination of and evidence for non-core-shell structure of particles containing black carbon using the Single-Particle Soot Photometer (SP2), *Geophys. Res. Lett.*., 39 (L06802), L050905, 2012.

Subramanian, R., Kok, G. L., Baumgardner, D., Clarke, A., Shinozuka, Y., Campos, T. L., Heizer, C. G., Stephens, B. B., de Foy, B., Voss, P. B., and Zaveri, R. A.: Black carbon over Mexico: the effect of atmospheric transport on mixing state, mass absorption cross-section, and BC/CO ratios, *Atmos. Chem. Phys.*, 10, 219-237, 2010.Wehner, B., Berghof, M., Cheng, Y. F., Achtert, P., Birmili, W., Nowak, A., Wiedensohler, A., Garland, R. M., Pöschl, U., Hu, M., and Zhu, T.: Mixing state of nonvolatile aerosol particle fractions and comparison with light absorption in the polluted Beijing region, *J. Geophys. Res*., 114 (D17): D010923, 2009.

Wiedensohle, A., and Fissan, H. J.: Bipolar Charge Distributions of Aerosol Particles in High-Purity Argon and Nitrogen, *Aerosol Sci. Technol.*, 358-364, 1991.

Zhang, R., Khalizov, A. F., Pagels, J., Zhang, D., Xue, H., and McMurry, P. H.: Variability in morphology, hygroscopicity, and optical properties of soot aerosols during atmospheric processing, Proc. Natl. Acad. Sci. USA., 105 (30), 10291-10296, 2008.